

https://doi.org/10.1070/QEL17958

Terahertz microscope with oblique subwavelength illumination: design principle

O.V. Minin, I.V. Minin

Abstract. **It is shown that the image contrast in the air when using a microscope based on dielectric microparticles with a size of the order of wavelength can be significantly enhanced with the help microparticles that provide the formation of the radiation localisation region at an angle to the direction of radiation incidence (at an angle to the optical axis). For this purpose, a screen is placed in front of the particle, which blocks part of the incident beam, forming a photonic hook or a photonic jet (terajet) with oblique illumination in the near field.**

Keywords: *photonic hook, photonic jet, terajet, oblique irradiation, image contrast.*

Conventional terahertz (THz) optical microscopes cannot resolve two objects located closer than $0.5\lambda/n\mathrm{NA}$ (λ is the wavelength of incident radiation, NA is the numerical aperture of the microscope, and n is the refractive index of the immersion medium), due to the Abbe diffraction limit. To overcome this fundamental limitation, many different approaches have been proposed [1–3], including an optical THz microscope based on microcavities [4], special mathematical image processing [5, 6], THz tomography [7], holography [8], the method of synthesised aperture [9, 10], and the use of structured fields [11, 12]. While these methods can achieve subwavelength resolution, they require time-consuming solutions to inverse problems. Systems implementing the principles of solid-state immersion in the THz range [13–16] and diffractive optics [17] are also promising.

In 2017, we demonstrated a method for increasing the spatial resolution of THz imaging systems by simply placing a dielectric mesoscale (comparable to the wavelength) particle in the focal region of the optical system of a THz microscope [18]. Since then, ultra-high-resolution THz imaging using dielectric microparticles has attracted considerable scientific interest due the simplicity of implementation and operation, as well as good compatibility with commercial microscopes. However, the superresolution mechanism underlying such methods is quite complicated and, apparently, is a combination of various effects: photonic nanojet (terajet), optical superresonances [19, 20], particle shape [21–23], illumination conditions and the substrate effect [24], which have been generalised in reviews, for example, in [25], and are still being investigated.

On the other hand, a well-known way to improve the resolution and contrast of an optical image is to use circular illumination [26, 27], although due to axial symmetry it does not give a strong pseudo-relief. In this case, oblique illumination of the object makes it possible to increase the optical image quality [28–30] by enhancing its contrast.

In this work, we propose the concept of a THz microscope combining these two approaches: the use of oblique illumination of an object by means of structured THz subwavelength fields in the near field in the form of a terajet and/or a photon hook [31, 32]. The key task for the implementation of this concept is to find the principle of constructing a particle that will ensure the formation of a photonic jet in the direction deviated from the direction of radiation incidence.

Mesoscale dielectric particles can generate a photonic hook due to their structural asymmetry [33], which is useful for improving contrast and image quality. The results obtained will contribute to the further development of methods of quasi-optical THz microscopy based on microparticles and facilitate their application in various fields – from biotechnology to nondestructive testing and life sciences.

With oblique illumination, the lens aperture is nonuniformly illuminated, which leads to a shadow image with enhanced resolution [28, 29]. To obtain such a nonuniform illumination, Abbe and Roy [34] proposed to move the condenser diaphragm to the side and thereby actually use a narrow axial illuminating beam instead of a wide one. Today, as such beams, it is advisable to use either photonic hooks or photonic jets (terajets) [31, 32] formed at an angle to the direction of radiation incidence on them (Fig. 1). In the case of axial formation of a photonic jet, the radiation is incident on the sample, and the diffracted –1st and + 1st orders are outside the particle boundary (Fig. 1a), while oblique irradiation leads to the fact that the diffracted +1st order is incident on a particle (Fig. 1b); as a result, this allows increasing the image contrast [30].

In work [33], one of the simplest methods of generating a photonic hook using a dielectric spherical or cylindrical particle was proposed, when part of the radiation incident on such a particle is shielded by an absorbing or metal screen installed in front of it. If the illuminating beam's width is less than the particle diameter, both components of the wave vector (parallel and perpendicular) do not compensate each other due to local destructive interference [33]. As a result, a photonic hook with a curvature proportional to the magnitude of the screened part of incident radiation is formed in the vicinity of the shadow part of the particle. In other words, only one part of the optical beam inside the microparticle is

O.V. Minin, I.V. Minin Tomsk Polytechnic University, prosp. Lenina 30, 634050 Tomsk, Russia,
e-mail: prof.minin@gmail.com, oleg.minin@ngs.ru

Received 27 August 2021
Kvantovaya Elektronika **52** (1) 13–16 (2022)
Translated by M.A. Monastyrskiy

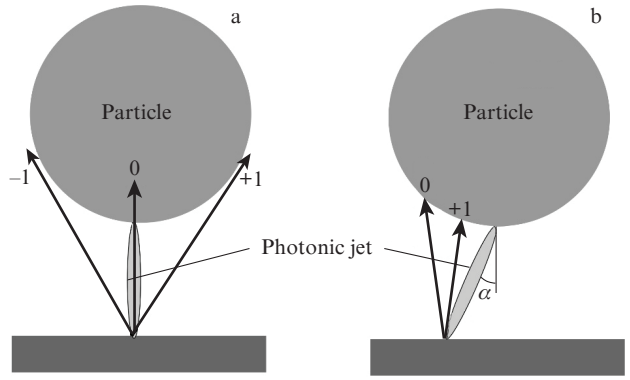

Figure 1. Scheme of a classical microscope (a) with a particle and (b) with oblique irradiation by a photonic jet or a hook. The numbers on the arrows indicate the diffraction order; α is the angle of inclination of the photonic jet to the optical axis.

refracted on its rear surface, as a result of which a curvilinear focusing zone – a photonic hook – is formed near the shadow surface of the microparticle.

Without reducing the generality of the problem, we briefly consider the formation of localised fields near the shadow surface of cylindrical and semi-cylindrical dielectric particles in the air, when a linearly polarised wave with a plane phase front is incident. The problem was simulated within the framework of the numerical solution of the wave equation for field vectors with the finite element method (FEM) using the Comsol Multiphysics program package. The incident plane wave had an initial amplitude of 1 V m^{-1} and propagated from left to right (Fig. 2). The minimum size of a triangular computational cell was $\lambda/(25n)$, where λ is the wavelength of the radiation incident on the particle, and n is the refractive index of the particle material. In order to implement free radiation conditions at the outer boundaries of the computational domain, a system of perfectly matched layers (PMLs) was used. To ensure maximum resolution using a photonic jet or a photonic hook formed by a dielectric particle, it is necessary that the field localisation region near the shadow boundary of such a particle is located near the particle–medium interface [33]. This is achieved by selecting the appropriate refractive index contrast, which in this case is equal to the refractive index of the particle material. The simulation results for two values of the particle's refractive index are shown in Figs 2 and 3, where the distributions of the squared electric field amplitude modulus are given.

Figures 2b and 2d show the formation of a photonic hook, the optical 'axis' of which is shifted from the symmetry axis and curved due to the incident beam asymmetry caused by the metal screen. Thus, one can see that shielding part of the wave front incident on a particle with a metal screen leads to a loss of energy, and the photonic hook intensity in the medium decreases. Nevertheless, the localised photon flux formed at the particle–medium interface is directed at an angle to the optical axis, which allows for oblique irradiation of the object under study.

The situation becomes more obvious in the case of using semi-cylindrical particles (Fig. 3). When the particle is fully irradiated, a photon jet is formed, localised along the particle's symmetry axis (Fig. 3a). With small screening of the irradiating beam, the photon hook effect manifests itself to the greatest extent, and a localised curvilinear region of space is formed near the particle's symmetry axis (Fig. 3b). With greater screening, an almost linear photonic jet is formed, directed from the particle's periphery to its optical axis, which allows for oblique irradiation of the object in the near field.

Figure 4 shows the angle of photonic jet deflection from the optical axis as a function of the degree of screening of the incident radiation (h/D) for a semi-cylindrical particle with the above parameters, where h is the screen height, and D is the particle diameter.

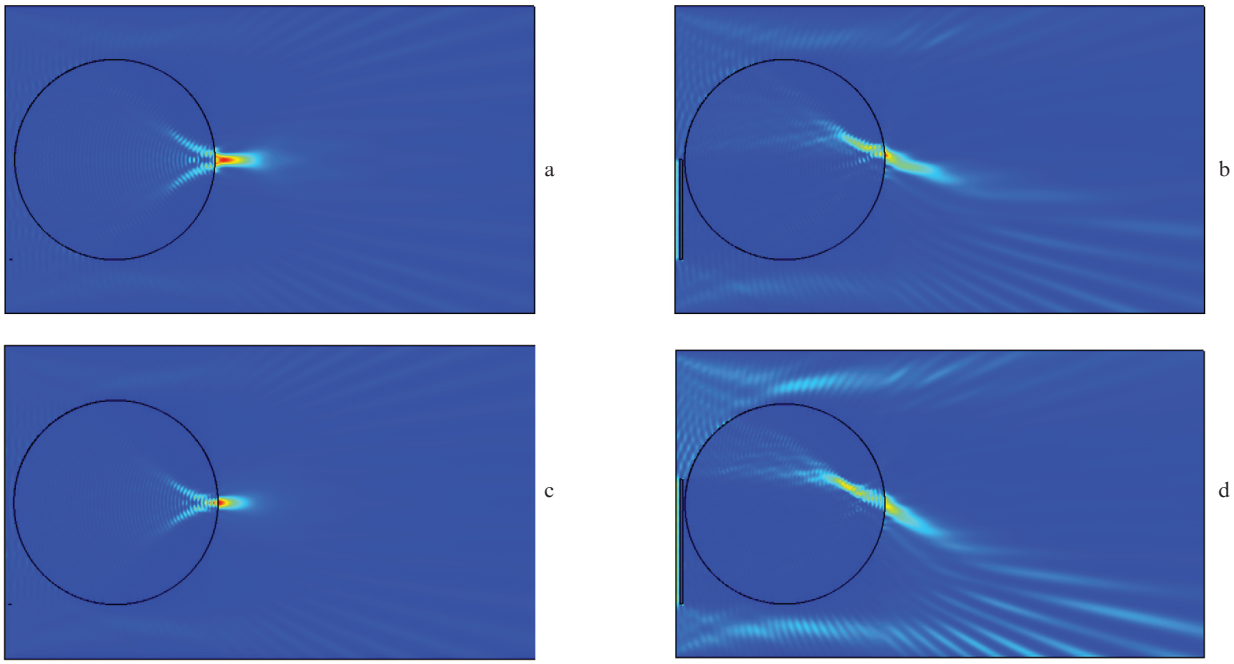

Figure 2. (Colour online) Formation of a photonic terajet and a photonic hook for a cylinder with a diameter of $D = 15\lambda$ with refractive indices of n = (a–b) 1.55 and (c–d) 1.8 in the air (a, c) without a screen and (b, d) with a screen.

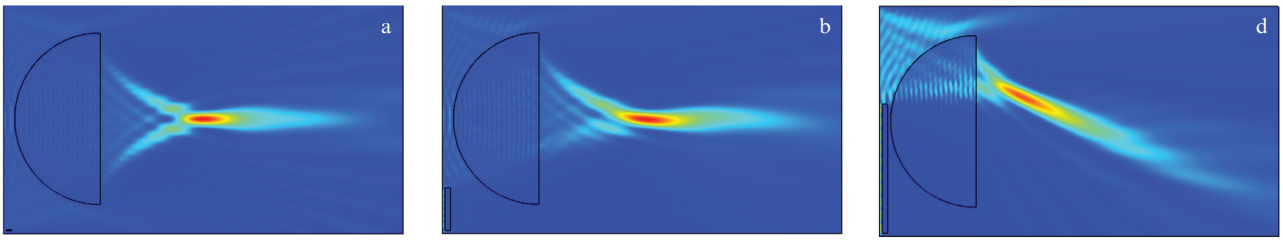

Figure 3. (Colour online) Formation of (a) a photonic terajet and (b, c) a photonic hook for a half-cylinder with a diameter of $D = 15\lambda$ with a refractive index $n = 1.45$ and various degrees of screening of incident radiation.

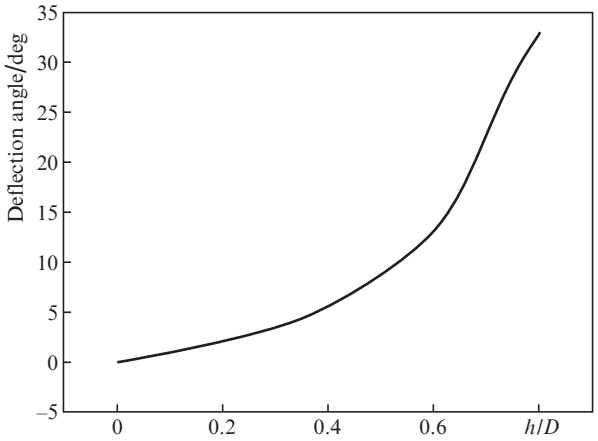

Figure 4. Angle of the photonic jet deflection from the optical axis at various degrees of screening of incident radiation for a semi-cylindrical particle with the parameters indicated in Fig. 2.

Preliminary experiments were conducted to test the proposed concept of a THz microscope with enhanced image contrast [35].

In work [36], a simple method was proposed for generating a photonic hook using a dielectric cubic particle with a metal screen installed along its side face. The photonic hook generation is based on controlling the tangential component of the electric field along the particle surface [37]. The corresponding problem was simulated numerically by solving Maxwell's equations using the CST Microwave Studio™ program package with a minimum cell size $\lambda/(25n)$, and $n = 1.46$ for teflon [38, 39]. Similarly to work [18], a cubic particle was placed in the air, had face dimensions equal to the radiation wavelength λ ($2.4 \times 2.4 \times 2.4$ mm) and was irradiated by a vertically polarised plane wave at a frequency of 125 GHz. In these studies, a metal (copper) screen with a length equal to half the length of the cubic particle edge and located along one of its lateral faces was used.

The conditions, scheme and parameters of the preliminary experiment were completely similar to those described in detail in Ref. [18]. Figure 5a shows the formation of a photonic hook, the optical path of which is shifted from the symmetry axis and curved due to the side metal screen. The localised photon flux formed near the particle's shadow surface is directed at an angle to the optical axis ($\alpha = 24°$), which allows for oblique irradiation of the object of study.

An aluminium grating with a thickness of 1 mm and a width of transparent grooves of 1.5 mm ruled at 1.5 mm was used as an object [18]. The image contrast C was determined by the well-known expression $C = (I_{max} - I_{min})/(I_{max} + I_{min})$, where I_{min} and I_{max} are the minimum and maximum amplitudes of the recorded signal [37, 40]. As follows from Fig. 5b, due to the use of oblique illumination with a photonic hook instead of axial illumination with a terajet, the image contrast increased by about 2.2 times.

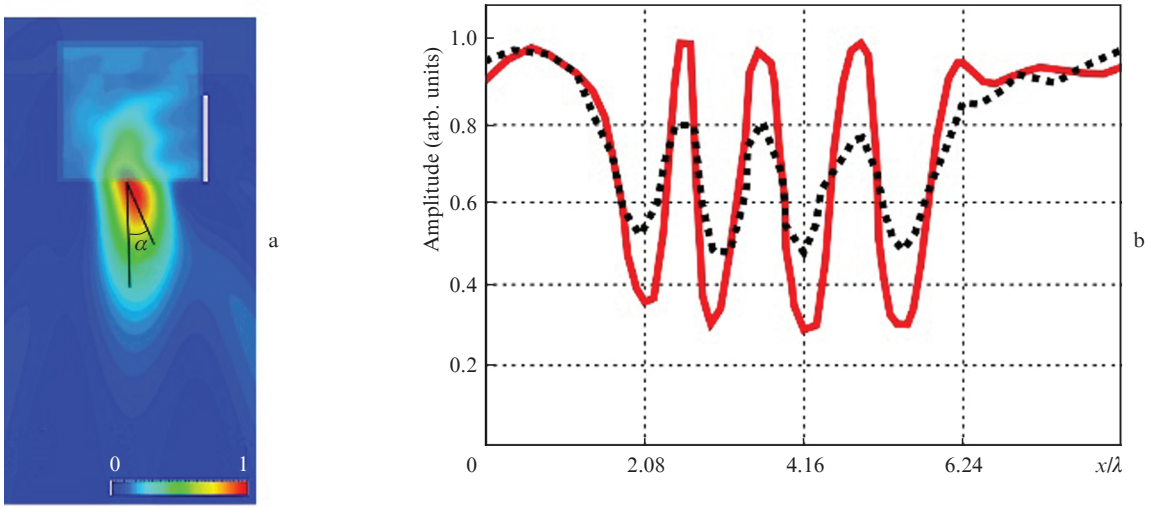

Figure 5. (Colour online) (a) Formation of a photonic hook by a cubic particle with a screen, and (b) the image contrast of a test-object with a terajet (dotted line) and a photonic hook (solid curve).

Oblique illumination in the near field can help the microscope lens to capture higher-order diffraction fields from the sample, which is important for improving the image quality and, first of all, its contrast in THz microscopes [41] based on microparticles, including for biophysical research [42]. This mechanism could play an important role in the development of more advanced and reliable imaging systems and ultra-high resolution microscopes. Optimisation of spatial resolution is achieved by a reasonable compromise between the particle size and its optical contrast. The same approach can be applied using other photonic hook generation methods discussed in detail in work [33], for example, for a combined particle of two or more dielectric materials.

Thus, we have shown the fundamental possibility of designing a microscope with oblique illumination in the near field, which allows one, without using an immersion medium (liquid), to obtain images with high contrast and ultra-high resolution inherent in photonic jets and terajets. This opens a new path to the development of more advanced and reliable THz imaging systems. In addition, given the scalability of Maxwell's equations [43], this approach can be used both in optics and acoustics [33, 44, 45].

Acknowledgements. This work was supported by the Tomsk Polytechnic University development programme.

References

1. Wai L., Chan J., Deibel D., Mittleman M. *Rep. Progr. Phys.*, **70**, 1325 (2007).
2. Guerboukha H., Nallappan K., Skorobogatiy M. *Adv. Opt. Photonics*, **10**, 843 (2018).
3. Akhmedzhanov I.M., Baranov D.V., Zolotov E.M., Shupletsova Yu.I. *Quantum Electron*., **49**, 698 (2019) [*Kvantovaya Elektron*., **49**, 698 (2019)].
4. Sulollari N., Keeley J., Park S., Rubino P., Burnett A., Li L., Rosamond M., Linfield E., Davies A., Cunningham J., Dean P. *APL Photonics*, **6**, 066104 (2021).
5. Ning W., Qi F., Liu Z., Wang Y., Wu H., Wang J. *IEEE Access*, **7**, 65116 (2019).
6. Ahi K. *IEEE T. Thz. Sci. Techn.*, **7**, 747 (2017).
7. Wang D., Li B., Rong L., Xu Z., Zhao Y., Zhao J., Wang Y., Zhai C. *Opt. Commun*., **432**, 20 (2019).
8. Valzania L., Zhao Y., Rong L., Wang D., Georges M., Hack E., Zolliker P. *Appl. Opt*., **58**, G256 (2019).
9. Krozer V., Loffler T., Dall J., Kusk A., Eichhorn F., Olsson R.K., Buron J.D., Jepsen P.U., Zhurbenko V., Jensen T. *IEEE Trans. Microw. Theory Techn*., **58** (7), 2027 (2010).
10. Valzania L., Zhao Y., Rong L., Wang D., Georges M., Hack E., Zolliker P. *Appl. Opt*., **58** (34), G256 (2019).
11. Shayei A., Kavenhash Z., Shabany M. *Appl. Opt*., **56** (15), 4454 (2017).
12. Olivieri L., Gongora J.S.T., Peters L., Cecconi V., Cutrona A., Tunesi J., Tucker R., Pasquazi A., Peccianti M. *Optica*, **7** (2), 186 (2020).
13. Pimenov A., Loidl A. *Appl. Phys. Lett*., **83** (20), 4122 (2003).
14. Gompf B., Gerull M., Muller T., Dressel M. *Infrar. Phys. Technol*., **49** (1–2), 128 (2006).
15. Kim S., Murakami H., Tonouchi M. *IEEE J. Sel. Topics Quantum Electron*., **14** (2), 498 (2008).
16. Chernomyrdin N., Kucheryavenko A., Zaytsev K., Kolontaeva G., Katyba G., Karalkin P., Smolyanskaya O., Karasik V., Minin O.V., Parfenov V., Gryadunova A., Norkin N., Minin I.V. *Proc. SPIE*, **10677**, 106771Y (2017).
17. Minin I.V., Minin O.V. *Proc. China-Japan Joint Microwave Conf*. (Shanghai, China, 2008). DOI: 10.1109/CJMW.2008.4772481.
18. Nguyen Pham H., Hisatake S., Minin O.V., Nagatsuma T., Minin I.V. *APL Photonics*, **2**, 056106 (2017).
19. Wang Z.B., Lukyanchuk B., Yue L., Yan B., Monks J., Dhama R., Minin O.V., Minin I.V., Huang S.M., Fedyanin A. *Sci. Rep*., **9**, 20293 (2019).
20. Yue L., Yan B., Monks J., Dhama R., Jiang C., Minin O.V., Minin I.V., Wang Z. *Sci. Rep*., **9**, 20224 (2019).
21. Geints Yu.E., Zemlyanov A.A., Panina E.K. *Quantum Electron*., **45** (8), 743 (2015) [*Kvantovaya Elektron*., **45**, 743 (2015)].
22. Yue L., Yan B., Monks J., Dhama R., Wang Z., Minin O.V., Minin I.V. *J. Infrar. Milli. Terahz Waves*, **39**, 546 (2018).
23. Cruz A., Cordeiro C., Franco M. *Proc. SPIE*, **9634**, 963412 (2015).
24. Minin O.V., Minin I.V. *Opt. Quantum Electron.*, **49**, 326 (2017).
25. Ma X., Jiang Z., Qu Q., Bin C., Zhenwei Z., Yuping Y. *Opto-Electron. Eng*., **47** (5), 190590 (2020).
26. Moon H., Yoon Y., Kim W., Park N., Park K., Park Y. *Opt. Express*, **18** (16), 17533 (2010).
27. Liau Z. *J. Appl. Phys*., **112**, 083110 (2012).
28. Valzania L., Zolliker P., Hack E. *Opt. Express*, **25**, 11038 (2017).
29. Sanchez C., Cristobal G., Bueno G., Blanco S., Borrego-Ramos M., Olenici A., Pedraza A., Ruiz-Santaquiteria J. *Micron*, **105**, 47 (2018).
30. Price J., Bingham P., Thomas E. *Appl. Opt*., **46** (6), 827 (2007).
31. Minin I.V., Minin O.V. *Diffractive Optics and Nanophotonics: Resolution Below the Diffraction Limit* (Springer, Cham, 2016).
32. Dholakia K., Bruce G.D. *Nat. Photonics*, **13**, 225 (2019).
33. Minin O.V., Minin I.V. *The Photonic Hook: From Optics to Acoustics and Plasmonics* (Springer, Cham, 2021).
34. Abbe E., Roy J. *Microscop. Soc. Ser. II*, **1**, 349 (1881).
35. Minin I.V., Minin O.V. *Preprints* 2021090024 (2021). DOI: 10.20944/preprints202109.0024.v1.
36. Liu C., Chen W., Minin O.V., Minin I.V. *Photonics*, **8**, 317 (2021).
37. Cremer C., Masters B.R. *Eur. Phys. J. H*, **38**, 281 (2013).
38. Kume E., Sakai S. *Meas. Sci. Technol*., **19**, 115501 (2008).
39. Rogalin V.E., Kaplunov I.A., Kropotov G.I. *Opt. Spektrosk*., **125** (6), 851 (2018).
40. Cakir S., Kahraman D.C., Cent-Atalay R., Cetin A.E. *IEEE Access*, **6**, 3839 (2018).
41. Zhang Y., Wang C., Huai B., Wang C., Zhang Y., Wang D., Rong L., Zheng Y. *Appl. Sci*., **11**, 71 (2021).
42. Formanek F., Brun M.A., Yasuda A. *Biomed. Opt. Express*, **2**, 58 (2011).
43. Vinogradov A.P., Aivazyan A.V. *Phys. Rev. E*, **60**, 987 (1999).
44. Ren X., Zhou Q., Xu Z., Liu X. *Appl. Phys. Express*, **13**, 064003 (2020).
45. Dholakia K., Drinkwater B.W., Ritsch-Marte M. *Nat. Rev. Phys.*, **2**, 480 (2020).